

NATIONAL AIR INTELLIGENCE CENTER



RESEARCH ON LASER-DAMAGE THRESHOLD OF PHOTOELECTRIC DETECTORS

by

Chen Dezhang, Zhang Cheng Quan, et al.

DTIC QUALITY INSPECTED 2



Approved for public release:
distribution unlimited

19960409 014

HUMAN TRANSLATION

NAIC-ID(RS)T-0007-96 21 March 1996

MICROFICHE NR: 960000262

RESEARCH ON LASER-DAMAGE THRESHOLD OF PHOTOELECTRIC DETECTORS

By: Chen Dezhang, Zhang Cheng Quan, et al.

English pages: 11

Source: Laser Technology, Vol. 19, Nr. 3, Jun 1995; pp. 135-140

Country of origin: China

Translated by: Leo Kanner Associates
F33657-88-D-2188

Requester: NAIC/TATD/Bruce Armstrong

Approved for public release: distribution unlimited.

<p>THIS TRANSLATION IS A RENDITION OF THE ORIGINAL FOREIGN TEXT WITHOUT ANY ANALYTICAL OR EDITORIAL COMMENT STATEMENTS OR THEORIES ADVOCATED OR IMPLIED ARE THOSE OF THE SOURCE AND DO NOT NECESSARILY REFLECT THE POSITION OR OPINION OF THE NATIONAL AIR INTELLIGENCE CENTER.</p>	<p>PREPARED BY: TRANSLATION SERVICES NATIONAL AIR INTELLIGENCE CENTER WPAFB, OHIO</p>
---	--

GRAPHICS DISCLAIMER

All figures, graphics, tables, equations, etc. merged into this translation were extracted from the best quality copy available.

RESEARCH ON LASER-DAMAGE THRESHOLD OF
PHOTOELECTRIC DETECTORS

Chen Dezhang, Zhang Cheng Quan, Qing
Guangbi, Liu Yun, Ye Zhusheng, Li Lin,
and Guo Yong

Southwest Institute of Technical Physics
Chengdu 610041

ABSTRACT: Permanent laser-damage effects in silicon PIN photoelectric diodes and silicon avalanche photodiodes irradiated with a 1.06 μm or an 0.53 μm laser are studied. The laser-damage thresholds of the detectors are experimentally measured. The main reason for causing permanent damage includes latent heat scorching at the PN junction of the photoelectric diodes. The damage thresholds are dependent on wavelength, pulse duration, and photodiode structure.

Key Words: photoelectric detector, permanent laser-damage threshold.

1. Introduction

Photoelectric detectors have widespread applications in military, civilian, and other areas owing to their high sensitivity, low noise, small bulk, and light weight. Yet they suffer from vulnerability to interference and damage when irradiated with an intense laser and therefore, research on their laser-damage effects and damage thresholds proves to be of practical importance. This paper focuses primarily on permanent

laser-damage effects on this kind of detector (including PIN photoelectric diodes and silicon avalanche diodes), as well as on measurement of their damage density thresholds.

2. Theory and Analysis

Permanent laser damage to photoelectric detectors is regarded as a kind of hard breakdown, in which detectors subjected to fatal destruction by a laser fail to operate normally and this damage cannot be erased. From experiments it was found that once a photoelectric detector is damaged by a laser, its performance deteriorates, such as a drop in response, an increase in dark current, a decrease in back resistance, and enhancement of noise. In our experiment, response R is taken as a measurable indicator of permanent damage, and permanent damage of a particular photoelectric detector can only be determined when its response drops to less than 20% of the original value under the condition of one-time damage. According to the working principles of silicon PIN photodiodes and silicon avalanche diodes, the two major processes in silicon PIN photodiode effects include the generation of photocarrier pairs and the separation of intense electric field from carriers, whereas the processes in silicon avalanche photodiode effects are represented by the generation of photocarrier pairs as well as the multiplication and separation of the PN junction avalanche region from carriers. The two processes as mentioned above are interdependent, that is, one cannot exist without the other. It is noted that the separation of carrier pairs during the photoelectric effect process is the most vulnerable situation. Permanent laser damage of a photoelectric detector is the capability of destruction during carrier separation, by which the detector capability to separate carrier pairs is weakened or even completely lost. As a result, the PN junction is destroyed and consequently, its carrier-collecting electric field becomes weak, too** simply, this electric field can hardly be built up. In response to this,

a damage mechanism is proposed, through which a dopant-enriched high-conductivity path is formed owing to the separation and redistribution of impurity atoms in a certain melting silicon material region. The further explanation of this mechanism is that a semiconductor, by absorbing light energy, can cause a temperature rise and when the temperature increases so much as to exceed the melting point, the material is melted and then quickly crystallizes upon cooling. During this process, high impurity atom concentrations are formed at the solid-liquid interface, which is in abrupt motion and these concentrations lead to the formation of the dopant-enriched high-conductivity path. If the path passes through the PN junction or if the PN junction is broken down by heat and fails to generate an intense electric field in order to collect carriers, then the photocarriers, although generated, cannot be collected in time and thereby cannot contribute to the photoelectric current. Even if the path just makes the PN junction narrower, it still can weaken the carrier-collecting electric field, as demonstrated by the drop in response. Similarly, when the impurity atoms concentrate to form a dopant-enriched high-conductivity path in a silicon avalanche photodiode, it may hinder the establishment of the avalanche-amplifying electric field as well, so that the avalanche diode may completely lose its function and there is no avalanche multiplication. And if the path passes through its PN junction, then the junction may also be broken down by heat just as happens in the case of PIN diodes and then it fails to collect carriers and gives no response to incident rays. It is noteworthy that the melting-point temperature at the PN junction of a photoelectric detector is a prerequisite to its permanent damage.

The laser heating effect, a major phenomenon arising from the interaction between laser and semiconductor, involves a process of generation, accumulation, and conduction of heat energy. Based on the equation of thermal conduction and the temperature distribution function of a transient ring-shaped heat

source acting on some semi-infinite solid surface [2], the temperature distribution function inside semiconductor T, under the action of a gaussian beam, can be calculated as follows:

$$T = \frac{ad^2(1-R')e^{-\alpha}P_0}{\sqrt{\pi Kk}^{-1/2}} \int_0^t \frac{P(t)dt}{t^{1/2}(4kt+d^2)} \exp\left[-\frac{z^2}{4kt} - \frac{r^2}{4kt+d^2}\right] \quad (1)$$

where α is the laser absorption coefficient of the material, R' is surface reflectivity, K and k are thermal conductivity and the coefficient of thermal expansion of the material, respectively, d is the flare radius time, P_0 is the peak power density, $P(t)$ is the pulse normalization function, t is the laser pulse action time, r and z are the cylindrical coordinate functions, respectively, r is the distance from the central shaft, and the starting point z is calculated from the incident face. Let r be zero, then the temperature distribution function T at the central shaft can be given by the following expression:

$$T_{\text{central shaft}} = \frac{2d^2P_0(1-R')e^{-\alpha}}{\sqrt{\pi Kk}^{-1/2}} \int_0^t \frac{P(t)dt}{t^{1/2}(4kt+d^2)} \exp\left(-\frac{z^2}{4kt}\right) \quad (2)$$

Since the melting-point temperature of the PN junction is a precondition for permanent damage to the photoelectric detector, if the distance of PN junction from the incident face is assumed to be a , and the melting point is assumed to be T_{th} , the permanent-damage peak power-density threshold and its energy-density threshold can be derived from Eq. (2), as follows:

$$\begin{cases} P_{th} = \frac{KT_{th}\sqrt{\pi}e^{-\alpha}}{ad^2\sqrt{k}(1-R') \int_0^t \frac{P(t)\exp(-a^2/4kt)}{t^{1/2}(4kt+d^2)} dt} \\ E_{th} = \frac{K\tau T_{th}\sqrt{\pi}e^{-\alpha}}{ad^2\sqrt{k}(1-R') \int_0^t \frac{P(t)\exp(-a^2/4kt)}{t^{1/2}(4kt+d^2)} dt} \end{cases} \quad (3)$$

where τ is the laser pulse half-duration. Eq. (3) shows that P_{th} , E_{th} is proportional to $e^{-\alpha a}$, that is, the larger the distance of the PN junction from the incident face, the more difficult the damage can be. And if the absorption coefficient α increases, the damage-density threshold will decrease. Thus, the damage-

density thresholds P_{th} , E_{th} , α , and τ are dependent on the structure of the photoelectric detector. To simplify Eq. (3), let $P(t)$ be continually equal to 1 and let a approach 0, P_{th} and E_{th} can be obtained as follows:

$$\begin{cases} P_{th} = K \sqrt{\pi} T_{th} / ad(1 - R') \text{arctg}(4k\tau/d^2)^{1/2} \\ E_{th} = K\tau \sqrt{\pi} T_{th} / ad(1 - R') \text{arctg}(4k\tau/d^2)^{1/2} \end{cases} \quad (4)$$

If $4k\tau \gg d^2$, $\text{arctg}(4k\tau/d^2)^{1/2}$ is approximately equal to $\pi/2$, then P_{th} and E_{th} are as follows:

$$\begin{cases} P_{th} = 2KT_{th} / ad(1 - R') \sqrt{\pi} \\ E_{th} = 2K\tau T_{th} / ad(1 - R') \sqrt{\pi} \end{cases} \quad (5)$$

If $4k\tau \ll d^2$, $\text{arctg}(4k\tau/d^2)^{1/2}$ is approximately equal to $4k\tau/d^2$, then P_{th} and E_{th} are as follows:

$$\begin{cases} P_{th} = dK \sqrt{\pi} T_{th} / 4ka(1 - R')\tau \\ E_{th} = dK \sqrt{\pi} T_{th} / 4ka(1 - R') \end{cases} \quad (6)$$

Eqs. (5) and (6) indicate that for detectors with the PN junction located at an extremely shallow portion of the incident face, their long pulse ($4k\tau \gg d^2$) damage-power-density threshold is not dependent on τ , while its energy-density threshold is in a direct ratio with τ . In the case of the short pulse ($4k\tau \ll d^2$), its power-density threshold is in inverse ratio to τ , while its energy-density threshold is not dependent on τ .

3. Experiment and Its Results

Fig. 1 shows a block diagram of the experimental principle. According to the diagram, an He-Ne laser is used to align and correct the optical path. The two experimental lasers used are at the wavelengths $1.06\mu\text{m}$ and $0.53\mu\text{m}$. The $1.06\mu\text{m}$ laser has pulse durations of 20ns and 60ns, while the $0.53\mu\text{m}$ laser has a pulse duration of 20ns. The adjustable laser power supply and neutral attenuators I and II are designed to adjust the incident laser damage energy. A sample plate and a laser energy meter are used

to perform incident-laser-damage energy. The sample-plate and laser-energy meter are used to perform real-time monitoring of

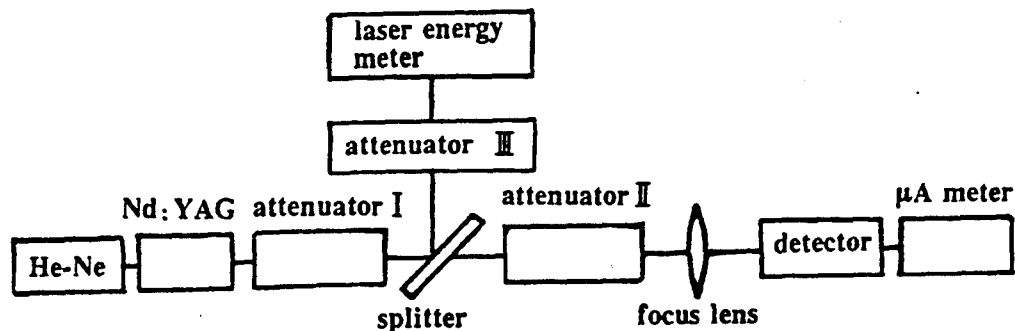


Fig.1 Experimental block diagram

incident laser energy. A focusing lens serves to converge beams with focal length 70 (1.06 μ m) and a precision microammeter is applied to monitor dark current. The photoelectric detectors used are SPD-001, SPD-002, and SPD-005 silicon photodiodes, and a SPD-032 silicon avalanche diode. The SPD-001 and SPD-002 have a p⁺p⁻n⁺ structure with a photosensitive surface 0.8mm, but the SPD-002 surface has undergone honeycomb processing. The SPD-005 has a p⁺n⁻n⁺ structure with a 3.5mmx3.5mm photosensitive surface. The SPD-032 has a p⁺pp⁻n⁺ with an 0.8mm photosensitive surface. During the experiment, the detectors are placed near the focal length of the focusing lens, the semi-intensive flare diameter at the location of the photosensitive surface is recorded on photographic paper, and the size of its scorch flare is measured with a reading microscope. The experimental result is shown in Table 1 and a comparison of detector performance before and after damage is listed in Table 2.

In the experiment, it was found that when a photoelectric detector is damaged with a 60 μ m laser pulse, its photosensitive surface exhibits regular circular fusion pits with much splash materials in the circumference and recrystallized mounds inside, as shown in Fig. 2. On the other hand, when a detector has

experienced permanent damage by a 20ns laser pulse, its photosensitive surface exhibits irregular shallow pits, normally vaporized pits where there are numerous extremely small mounds probably due to partial vaporization, and loud burst sounds are heard, accompanied by the appearance of cracks on the surface, as demonstrated in Fig. 3. A test of the detector I-V characteristics led to the discovery that they have departed widely from those of the diode; the back resistance decreased by several orders of magnitude, and even the PN junction turned into a pure resistance feature and as a result, the PN junction of the photodiode has been severely damaged and the response was substantially reduced or completely disappeared. In the event that the detector has gone through permanent damage with an 0.53 μ m laser, its photosensitive surface shows damage spots instead of damage pits without clear burst sounds as exhibited in Fig. 4.

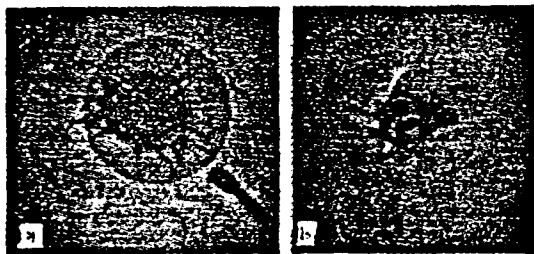


Fig.2 Photograph of the surface of the damaged detector by 1.06 μ m, 60 μ s laser pulse ($100\times$)
a - SPD-001 100times b - SPD-005 100times

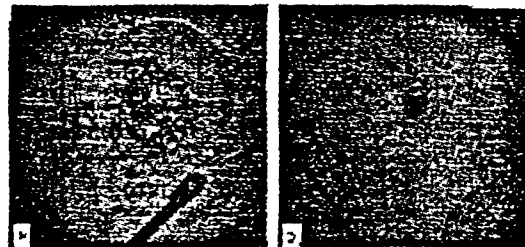


Fig.3 Photograph of the surface of the damaged detector by 1.06 μ m, 20ns laser pulse($100\times$)
a - SPD-032 100times b - SPD-005 40times



Fig.4 Photograph of the surface of the damaged detector by 0.53 μ m, 20ns laser pulse ($40\times$)

4. Conclusions and Analysis

1. The perpetual laser damage of a photoelectric detector is virtually thermal damage, which is accompanied by stress, fusion, and vaporization with cracks, splash material-surrounded fusion pits, and vaporized pits emerging on the photosensitive surface. In addition to these, response deteriorated to such a degree that the detector hardly shows any response to incident rays.

2. The permanent damage excited by a laser in the photoelectric detector is breakdown on its PN junction, because of which the dopant-enriched high-conductivity region may form due to a high concentration of impurity atoms. As a result, the PN junction becomes narrower or even broken down by heat and the carrier-collecting intensive electric field or avalanche electric field becomes weak or even cannot be built up. It is therefore believed that the location of the PN junction has a rather strong effect on the damage resistance of a photoelectric detector. In the SPD-001 and the SPD-032, the PN junction, located in the deep section of the incident face shows the highest damage threshold and furthermore, the value is approximately identical in both cases to imply that their structures are similar, too. In the SPD-005, however, the PN junction is situated in the shallow part of the incident face and thus, its damage threshold turns out to be smaller. Obviously, the foregoing analysis suggests that the experimental data closely fit the theoretical values.

3. As for photoelectric detectors such as the SPD-001 and the SPD-032, with the PN junction located in the deep part of the incident face, the damage-energy threshold from a 20ns laser appears slightly larger than for a 60ps laser. This is so because the interaction process of the 20ns high-powered laser and semiconductor gives rise to the generation of plasma, which, by absorbing light energy, serves as a kind of protection. Nevertheless, in the SPD-005 photodiode, the energy-density

thresholds derived under the action of the above two laser pulses exhibit not much difference, while the power-density threshold acquired under the action of a short pulse proves to be much larger. The reason for this situation is that in the SPD-005 photodiode, the PN junction is located in the extremely shallow section of the incident face, that is, a approaches 0, so that it can satisfy the condition of $4k\tau \ll d^2$ for both the 20ns and the 60 μ s pulses. From Eq. (6) we know that E_{th} is not dependent on τ ; P_{th} is proportional to r^{-1} . It is clear that the experimental data agree with the theoretical values.

4. The damage-density threshold for an 0.53 μ m laser is much smaller than in the case of a 1.06 μ m laser, because the absorption coefficient of the semiconductor material is much larger for the 0.53 μ m laser than for the 1.06 μ m laser.

The foregoing discussion leads to the conclusion that the laser damage-density thresholds of the photoelectric detectors are dependent on wavelength λ , pulse duration τ , and detector structure.

Our special thanks are due to research fellows Yang Qingchu, Wen Xuedong, and Huo Lianzheng, and to senior engineers Pu Shude and Guo Xizhen, for their assistance and advance.

On the authors: Zhang Guowei, male, born in March 1933, is a professor who formerly was a visiting scholar at the Berlin Technical University, Germany. Currently, he is engaged in many research projects including tunable dye lasers, transition-metal-ion (solid-state tunable) lasers, spectroscopic technology, applied laser spectral technology, and infrared waveguides.

Chen Dezhang, male, born in November 1964, holds the master of science degree and has been involved in research on laser technology.

Table 1 Damage density threshold for photo-electric detector

wavelength (μm)	pulse- width	number	diameter (mm)	energy density threshold (J/cm^2)	power density threshold (W/cm^2)	phenomenon
1.06	20ns	SPD-001-12	$\varnothing 0.8$	64.8	3.23×10^9	the surface of detectors are marked by small mounds and irregular shallow pit. The loud burst sounds are heard.
1.06	20ns	SPD-005-10	3.5×3.5	31.5	1.58×10^9	the same above
1.06	20ns	SPD-005-21	3.5×3.5	26.8	1.32×10^9	the same above
1.06	20ns	SPD-032-7	$\varnothing 0.8$	64.3	3.22×10^9	the same above
1.06	$60\mu\text{s}$	SPD-001-13	$\varnothing 0.8$	43.7	7.28×10^5	the surface of detectors are marked by deeper circular pit resolidified mounds and splash material. No burst sounds
1.06	$60\mu\text{s}$	SPD-001-15	$\varnothing 0.8$	42.3	7.05×10^5	the same above
1.06	$60\mu\text{s}$	SPD-002-5	$\times 0.8$	32.4	5.40×10^5	the same above
1.06	$60\mu\text{s}$	SPD-005-9	3.5×3.5	36.3	6.05×10^5	the same above
1.06	$60\mu\text{s}$	SPD-032-8	$\varnothing 0.8$	47.6	7.93×10^5	the same above
0.53	20ns	SPD-001-11	$\varnothing 0.8$	5.6	2.80×10^8	the photo-sensitive surface of detectors are marked by white damage spot. No burst sounds
0.53	20ns	SPD-032-4	$\varnothing 0.8$	4.92	2.46×10^8	the same above

Table 2 Characteristics comparison of photo-electric detector

Number	before damage				after damage			
	I_d (nA)	R_1 (Ω)	R_2 ($M\Omega$)	responsivity (A/W)	I_d (mA)	R_1 (Ω)	R_2 (Ω)	responsivity (A/W)
SPD-001-12	20	300	>20	0.16	2.0	10	10	No singal
SPD-005-10	8	85	>20	0.79	4.0	43	43	0.026
SPD-005-21	9	85	>20	1.5	1.4	85	2.0×10^3	0.228
SPD-032-7	60	80	>20	>11	2.0	75	5.5×10^3	No singal
SPD-001-13	10	100	>20	0.17	4.0	7	7	No singal
SPD-001-15	20	80	>20	0.15	2.8	72	5.5×10^4	No singal
SPD-002-5	10	95	>20	0.53	4.0	10	10	No singal
SPD-005-9	18	150	>20	0.74	4.0	20	20	No singal
SPD-032-8	60	80	>20	>11	2.0	44	44	No singal
SPD-032-4	60	85	>20	>11	1.5	80	6.2×10^3	No singal
SPD-001-11	10	85	>20	0.16	2.0	84	9.0×10^3	No singal

The paper was received on July 27, 1994.

PRODUCT PREVIEW

DIODE PUMP LASER

The MicraChip MC-22 laser, developed by Micracor, Inc., Massachusetts, can be applied to analog-to-digital optical fiber communication and RF networks. It is characterized by transmission output >100mW, wavelength 1319nm, and high-quality TEM₀₀ laser beams. The Nd:YAG crystal used for the diode pump is well packed in the manufacturing plant, with several optical cable lead wires of different sizes. When the linearly-polarized MicraChip is coupled with signal-transmitting external modulator, the output power of the device exceeds that of laser diode systems by a factor of 5. The noise-suppressing circuit can ensure a low-distortion transmission applied to CATV. When the MC-22 relative luminance noise exceeds 10MHz, the related value is lower than 165dB/Hz. The working power supply of this laser is 5V, 3A.

Reported by Yu Zhulan and Cao Sansong

DISTRIBUTION LIST

DISTRIBUTION DIRECT TO RECIPIENT

<u>ORGANIZATION</u>	<u>MICROFICHE</u>
BO85 DIA/RTS-2FI	1
C509 BALL0C509 BALLISTIC RES LAB	1
C510 R&T LABS/AVEADCOM	1
C513 ARRADCOM	1
C535 AVRADCOM/TSARCOM	1
C539 TRASANA	1
Q592 FSTC	4
Q619 MSIC REDSTONE	1
Q008 NTIC	1
Q043 AFMIC-IS	1
E404 AEDC/DOF	1
E410 AFDTC/IN	1
E429 SD/IND	1
P005 DOE/ISA/DDI	1
1051 AFIT/LDE	1
PO90 NSA/CDB	1

Microfiche Nbr: FTD96C000262
NAIC-ID(RS)T-0007-96